Photochemistry and Photobiology, 2002, 76(4): 438–445

Preclinical Studies in Normal Canine Prostate of a Novel Palladium-Bacteriopheophorbide (WST09) Photosensitizer for Photodynamic Therapy of Prostate Cancer¶

Qun Chen*[1], Zheng Huang[1], David Luck[1], Jill Beckers[1], Pierre-Herve Brun[2], Brian C. Wilson[3], Avigdor Scherz[4], Yoram Salomon[4] and Fred W. Hetzel[1]

[1]HealthONE Alliance, Denver, CO;
[2]Steba Biotech, Toussus-Le-Noble, France;
[3]Ontario Cancer Institute, University of Toronto, Toronto, Canada and
[4]Weizmann Institute of Science, Rehovot, Israel

Received 24 April 2002; accepted 22 July 2002

ABSTRACT

Photodynamic therapy (PDT) uses light to activate a photosensitizer to achieve localized tumor control. In this study, PDT mediated by a second-generation photosensitizer, palladium-bacteriopheophorbide WST09 (Tookad) was investigated as an alternative therapy for prostate cancer. Normal canine prostate was used as the animal model. PDT was performed by irradiating the surgically exposed prostate superficially or interstitially at 763 nm to different total fluences (100 or 200 J/cm^2; 50, 100 or 200 J/cm) at 5 or 15 min after intravenous administration of the drug (2 mg/kg). Areas on the bladder and colon were also irradiated. The local light fluence rate and temperature were monitored by interstitial probes in the prostate. All animals recovered well, without urethral complications. During the 1 week to 3 month post-treatment period, the prostates were harvested for histopathological examination. The PDT-induced lesions showed uniform hemorrhagic necrosis and atrophy, were well delineated from the adjacent normal tissue and increased linearly in diameter with the logarithm of the delivered light fluence. A maximum PDT-induced lesion size of over 3 cm diameter could be achieved with a single interstitial treatment. There was no damage to the bladder or rectum caused by scattered light from the prostate. The bladder and rectum were also directly irradiated with PDT. At 80 J/cm^2, a full-depth necrosis was observed but resulted in no perforation. At 40 J/cm^2, PDT produced minimal damage to the bladder or rectum. On the basis of optical dosimetry, we have estimated that 20 J/cm^2 is the fluence required to produce prostatic necrosis. Thus, the normal structure adjacent to the prostate can be safely preserved with careful dosimetry. At therapeutic PDT levels, there was no structural or functional urethral damage even when the urethra was within the treated region. Hence, Tookad-PDT appears to be a promising candidate for prostate ablation in patients with recurrent, or possibly even primary, prostate cancer.

INTRODUCTION

In the United States, prostate cancer is the most common cancer in men, and the second leading cause of cancer death among them (1). Although there are only palliative treatments for metastatic prostate cancer, early-stage prostate cancer is often confined within the organ and is treated with curative intent by surgery, radiation therapy (brachytherapy, external beam or a combination of both), or by both surgery and radiation, which offer a cure rate ranging from 50% to 70% (2–4). Significant side effects are reported to be associated with these current therapies. Approximately half of the patients suffer from impotency after either radiation or surgery (4,5). Other severe complications include urinary incontinence and injuries to nearby structures after radical prostatectomy (surgical removal of prostate), and bladder and bowel dysfunction after radiation therapy. Hyperthermia has been used in both benign hyperplasia and cancer of the prostate, primarily to relieve the urinary symptoms. The outcomes of the treatments appear to be modest (6). The primary limitation of hyperthermia is the difficulty in achieving a temperature (in the prostatic tissue) high enough to cause direct cell killing, using current technologies for energy delivery devices. Other drawbacks are that several sessions are required to provide even temporary relief of the symptoms, and there is the potential to develop prostatorectal fistula (6). Image-guided cryotherapy provides another option for the treatment of primary prostate cancer. But available data indicate that the results of cryotherapy are comparable with those of both radiotherapy and radical prostatectomy (7). High-intensity focused ultrasound (HIFU) is a minimally invasive technique and can induce thermal lesions at depths >10 cm. Preliminary results showed that transrectal HIFU could induce partial ablation with high rates of negative biopsies, low prostate-specific antigen and a low complication rate, although some patients might need transurethral debris resection

¶Posted on the website on 25 July 2002.
*To whom correspondence should be addressed at: HealthONE Alliance, 1850 High Street, Denver, CO 80218, USA. Fax: 303-320-6018; e-mail: pdtlaser@aol.com
Abbreviations: Deff, effective attenuation depth; H&E, hematoxylin and eosin; HIFU, high-intensity focused ultrasound; i.v., intravenous; PDT, photodynamic therapy; SQ, subcutaneous; Tookad, palladium-bacteriopheophorbide, WST09.

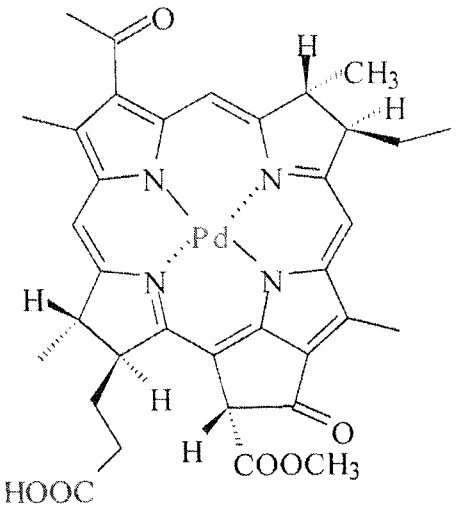

Figure 1. Molecular structure of Tookad.

(8). There is still a need for an alternative or adjunctive therapy to treat localized prostate cancer, either as a primary modality or as a postradiation failure.

Photodynamic therapy (PDT) is an evolving cancer treatment modality. The procedure involves administration of a light-sensitive drug (photosensitizer). A time is allowed for the drug to be taken up in the target tissue that is then irradiated with light of appropriate wavelength to activate the photosensitizer. This initiates a sequence of photochemical, chemical and biological reactions, which ultimately lead to cell death (9). PDT using the first-generation photosensitizer Photofrin (Axcan, Montreal, Canada) has been approved by the U.S. Food and Drug administration for treatment of selected types of tumors such as esophageal and lung cancers. The feasibility of using PDT on animal models to treat prostate cancer has been investigated in this laboratory as well as in several others. There are several reports of PDT in a rat prostate tumor model, which indicate that PDT can effectively kill prostate tumors (10–14). Canine prostate has been used as an animal model for studying PDT in prostate because of its resemblance both in physical size and in anatomical structure to that of humans. *In vivo* optical properties of canine prostate have been studied for Photofrin-mediated PDT in this laboratory and were found to be similar to those of *in vivo* human prostate (15–17). Canine prostate tissue responses to PDT mediated by various photosensitizing agents were investigated (18–22), and the general consensus is that, given a fixed optical dose, the volume of tissue damage is rather unpredictable.

The present work is a pilot study using a second-generation photosensitizer, palladium-bacteriopheophorbide, WST09 (Tookad; Steba Biotech, Toussus-Le-Noble, France), to ablate prostatic tissue. Tookad is a novel and pure palladium-substituted bacteriochlorophyll derivative (Fig. 1). It has a maximum absorption wavelength in the near-infrared (763 nm) with a high extinction coefficient ($\varepsilon = 10^5$ mol^{-1} cm^{-1} in chloroform [23]). The drug has extremely fast pharmacokinetics—cleared rapidly from the circulation (95% in 15 min in mice) and from other tissue in the order of a few hours (A. Scherz, personal communication). Its effectiveness on human prostatic small-cell carcinoma has been demonstrated on a mouse xenografts model (Y. Salomon, personal communication).

The objectives of this study were to (1) demonstrate that Tookad-PDT can destroy a clinically significant volume of prostate tissue; (2) determine the optimum drug–light time interval; (3) assess the dependence of the size of the PDT lesion on the light dose; and (4) determine the potential phototoxic damage to adjacent tissues and normal prostatic structures, including the bladder, rectum and urethra, and thereby evaluate the potential effectiveness and morbidity of the treatment. Because the ultimate clinical objective requires that the whole prostate be treated because of the poor differentiation from normal tissue and the multinodular nature of prostate cancer, it was critical for this study to use a large-animal model in which the size of the prostate is similar to that in humans. Hence, canines were selected. The limitation is that there is no readily available prostate cancer model in the canine (other than serendipitous spontaneous disease). Hence, the study reports only on the response of normal prostate tissue. But there are reports indicating that, if all other treatment parameters are identical, PDT is likely to be equally effective in destroying normal tissue and the embedded cancerous tissue from the same tissue origin (24–29). Again, given that the selective destruction of tumor is not an absolute prerequisite for PDT to be applied successfully in patients, the results obtained are directly useful for the design of clinical trials.

MATERIALS AND METHODS

Animal model. A total of 16 adult healthy Beagles (2–8 years old, 14–18 kg) were studied. The animals were obtained from licensed vendors (Marshall Farm, North Rose, NY, or Harlan Farm, Indianapolis, IN) and conditioned for a minimum of 1 week before any experimental procedures were carried out. All studies were performed under the guidance of the Institutional Care and Use Animal Committee at HealthONE Alliance. The prostate in these animals is typically ~3 cm in lateral diameter. Benadryl (intravenous [i.v.] 0.7–1.4 mg/kg) and dexamethasone (subcutaneous [SQ], 2 mg/dog) were given immediately before the start of photosensitizer infusion to counteract the effect of the cosolvent Cremophor EL on blood pressure.

Photosensitizer. Tookad is not water soluble and so was prepared in a Cremophor EL–based vehicle (Sigma Diagnostics, St. Louis, MO) by the manufacturer. The concentration of Tookad (5 mg/mL) was determined spectroscopically at 763 nm using an extinction coefficient of 10.86×10^4, an assumed number upon dilution in chloroform. The drug was given to the animal at a dosage of 2 mg/kg by slow i.v. infusion under dimmed ambient lighting.

Light source, light delivery and detection fibers. The light source was a portable 763 nm diode laser (CeraLas; CeramOptec, Bonn, Germany) with a maximum output power of 4 W and a calibration port for determining delivered output power. The laser output was directly coupled with a series of beam splitters that allowed up to four irradiation fields to be treated simultaneously. The light fluence rates were $\leqslant$150 mW/cm^2 for the surface irradiation fields delivered through microlens fiber (Model FD; Medlight S.A., Ecublens, Switzerland) and $\leqslant$150 mW/cm for diffusing fiber for interstitial irradiations delivered through cylindrical diffuser fiber (10 mm active length, 1.3 mm diameter; Model CD 603-10C; CeramOptec).

To monitor the dynamics of light fluence within an irradiated prostate, optical fibers with an isotropic scattering tip were used as light detectors. The probes were implanted into the prostate at predetermined positions, and the output was coupled with a photometer (Model 88XL; Photodyne, Westlake Village, CA). The meter was reset before each irradiation session to compensate the ambient light. The acquired data were corrected for the probe transmission rates.

A custom-made adjustable template attached to a pole and centered over the prostate was used for guiding the placement of fibers. Effective attenuation depth (Deff), defined as the linear distance required for light fluence rate to decrease by a factor of 1/e (approximately 37%), was derived as

$$\text{Deff} = 3/\ln(\phi_3/\phi_6) \quad (1)$$

where ϕ is the fluence rate at each radial distance.

Table 1. Treatment scheme

Case no.	Drug–light interval (min)	Prostate*		Bladder surface (J/cm^2)	Colon surface (J/cm^2)	Survival time (weeks)
		Superficial (J/cm^2)	Interstitial (J/cm)			
1		No drug, no light				0
2	No drug	200	200			1
3		No light. Full surgical procedures were performed.				12
4†	15	200	200		10, 20‡	1
5†	15	200	200	20	40	1
6†	15	200	200	40	40	1
7	15	100	100	40	40	1
8	15	100	100	40	80	1
9	15	100	100	40	80	1
10	15	200	200			1
11	15		100, 200			12
12	15		50, 200			4
13	15		50, 50			1
14	5		100, 200			1
15	5		50, 200			1
16	5		50, 100			1

*One lobe was treated by surface irradiation and one by interstitial irradiation, or both lobes by interstitial.
†Rectum was stitched to the prostate.
‡On different sites.

Surgical and PDT procedures. Standard sterilization procedures were strictly followed. All surgical instruments and invasive probes were either autoclaved or chemically sterilized. As an extra precaution, the dogs received antibiotics before and after surgery (intramuscular, ampicillin, 20 mg/kg) to prevent possible infection. Pain control consisted of preoperative and postoperative injection of morphine, with long-term control provided by Fentanyl patches.

The dogs were prepared for surgery according to a standard canine laporatomy procedure. An incision was made midway between the costal margin and the umbilicus to the pubic symphysis. The connective and fat tissues around the prostate were dissected to expose the anterior and lateral prostate surfaces. Extra caution was taken during this step to preserve the nerves. Once exposed, the prostate gland was raised for easier access by padding sterilized gauze under it. In some animals the underlying rectum was stitched directly to the prostate capsule to more closely simulate human anatomy. The optical fibers for PDT irradiation and for *in situ* optical measurements were positioned at predetermined locations before drug infusion. For surface irradiation, a 1 cm diameter light field was centered on one prostate lobe, the center of the bladder and one or two sites on the colon. Surface irradiation was delivered from outside the prostate capsule, and both the bladder and the colon were irradiated from serosal surfaces. For interstitial irradiation, a 1 cm diffuser was inserted into the opposite lobe after making an insertion channel using an angled micropick (1 mm) and a cone-shaped dissecting probe (1.5 mm). The light fluence probes were placed 3 or 6 mm radially from the interstitial fiber. Thermocouples (0.5 mm diameter; Oxford Optronix Ltd., Oxford, UK) for temperature monitoring during irradiation were placed 3 mm radially from the interstitial source fiber or 1 mm below the irradiated surface. Because we observed no tissue temperature changes in the initial several animals during light irradiation, the temperature measurement was eliminated in further studies to reduce the possible mechanical damages associated with the probe insertion.

Tookad (2 mg/kg) was administered by slow infusion through an i.v. catheter at a rate of 0.5 mL/min for a period of 10–14 min. Light was applied 5 or 15 min after completion of the infusion. For surface irradiation of the prostate, the radiant exposure was either 100 or 200 J/cm^2, and for interstitial irradiation, 50, 100 or 200 J/cm was delivered. In addition to and simultaneous with the direct irradiation of the prostate, a 1 cm diameter spot on both the bladder and the colon was superficially irradiated up to 80 J/cm^2 using separate optical fibers. Irradiation lasted 8–23 min in each animal. The details of the treatments given to each dog are listed in Table 1.

Immediately after light irradiation, the rectus muscle, fascia and skin were closed with interrupted sutures. The endotracheal tube was removed on recovery of the swallow reflex. The i.v. catheter was removed, and an Elizabethan collar was placed around the dog's neck to prevent it from licking the incision site. Standard procedures were followed for animal care, including continued pain control. Urinalysis was performed before and after treatment (24–48 h) for four dogs. After surgery, the dogs were kept in dimmed ambient lighting for 2–4 h. The PDT-treated animals and control animals (light only or drug only) were killed at predetermined time points (1 week, 1 and 3 months) after PDT, using barbiturate overdose.

Histopathological examination. At necropsy, the prostate, bladder, underlying rectum and section of treated colon were removed and photographed. The prostate was dissected from the urinary bladder. All specimens were fixed in 10% neutral buffered formalin. The prostate, bladder and colon were cut into 3 mm blocks, photographed and embedded in paraffin. Sections of 5 μm thickness were stained with hematoxylin and eosin (H&E) and Dyer's Verhoeff Variation (30) to examine the histopathological changes.

RESULTS

Thermal effects

During the 150 mW/cm^2 surface or 150 mW/cm interstitial irradiation, the measured temperature rose by a maximum of 0.9°C at 1 mm below the irradiated surface or 3 mm radially from the interstitial source, respectively. It is therefore concluded that the observed tissue damage described below was the result of PDT rather than of heat. This was further confirmed by the absence of damage in the control prostate that received light irradiation but not photosensitizer, even though the light was at a higher fluence rate of 200 J/cm^2 or 200 J/cm. Also, no damage was found near the interstitial source or at the irradiated surface.

Dynamic light fluence measurements during PDT

Figure 2 is a representative plot of the relative light fluence as a function of time during the treatment, measured at the fixed locations in the vicinity of the interstitial irradiation source. In the monitored animals, the Deff, as defined in Materials and Methods, was stable within 36% during irradiation (17 $\pm$ 21%, n = 12). It was noticed that there was a case in which the light fluence rate increased in value during irradiation. It is likely that probe movement during the measurement could result in some of

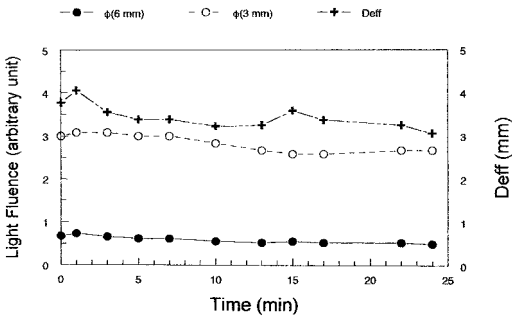

Figure 2. Relative light fluence rate measured at 3 and 6 mm radially from the irradiation source and the derived Deff during a 763 nm Tookad-PDT (2 mg/kg, irradiation started 15 min after completion of drug administration).

the larger variations in light fluence measurement. Hence, even though Tookad acts primarily as a vascular-targeted photosensitizer, the vascular response during treatment, along with the mechanical damage induced by optical probe insertion, did not produce any significant change in the light distribution. The stability in the tissue optical property of Tookad-PDT is most likely because of the long-wavelength activation, for which the absorption of blood is relatively small. This contrasts with the substantial variations both between subjects and as a function of time during similar PDT studies using Photofrin at 630 nm (6,15,16). The finding suggests a simpler optical dosimetry for Tookad-PDT in the prostate, compared with that at shorter activation wavelengths.

Postsurgical observations

All control animals that received either light only or drug only and animals that received PDT survived the 1 week to 3 month postsurgical period without incident. None of the dogs showed urinary retention, and urinary catheterization was not needed. Urinalysis was performed for one control (drug only) and three treated dogs (receiving 50, 100 and 200 J/cm, respectively); all had trace amounts of blood in the urine within the first 24–48 h. None required medical attention or treatment. The surgical wound healed well in all treated dogs, with no postsurgical urethral complications.

Macroscopic findings

The control group had two dogs. One received light-only treatment and was euthanized after 1 week. The other received drug treatment only and was euthanized after 3 months. Both prostates showed no abnormalities. No noticeable mechanical damage at the sites of insertion of the light delivery, the detector fibers and the thermocouple was seen.

In six dogs, each lobe received single interstitial irradiation, whereas in another seven, each prostate received surface irradiation on one lobe and interstitial treatment in the other lobe. One week after treatment, the PDT-induced lesions were characterized by acute hemorrhagic necrosis with patchy subcapsular hyperemia and marked edema, as seen in the representative gross section shown in Fig. 3. The PDT-induced lesions were well delineated from the adjacent normal tissue, and the zone of necrosis increased with the increase in the delivered light fluence. The boundary of the lesions was sharply defined, consistent with there being a PDT-response threshold, as reported with other photosensitizers (6,15,16,31). The lesions were centered on the

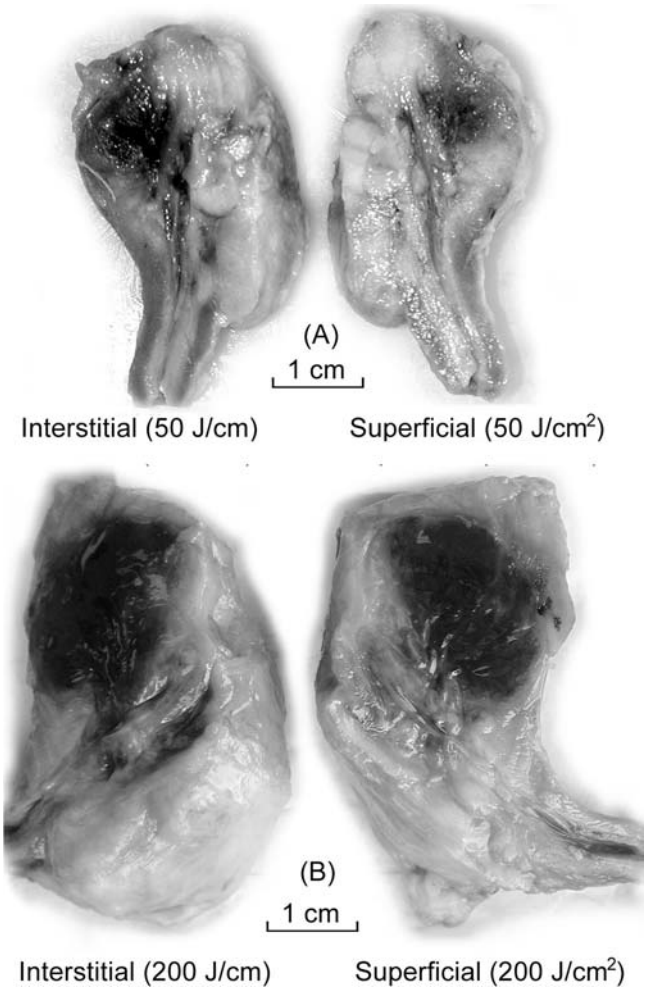

Figure 3. Cross-view of prostate 1 week after PDT (2 mg/kg, 15 min drug–light interval) consisting of lateral sections from the two sides of the prostate, cut through the midline. A: The right lobe received 100 J/cm interstitial irradiation and the left lobe 100 J/cm^2 surface irradiation. B: The right lobe received 200 J/cm interstitial irradiation and the left lobe 200 J/cm^2 surface irradiation. The increase in the zone of necrosis correlated well with delivered light fluence. The overlapping of the lesions was seen along the midline cutting.

treatment fiber and entirely within the lobe or reached the boundary of the treated prostate. The capsular and urethral structures appeared intact. The size of the lesions was determined by the number of dissected sections containing necrotic lesions. The orthogonal diameters of lesion on each dissected section were also measured. As seen in Fig. 4, the lesion diameter increased approximately linearly with the logarithm of the light fluence, consistent with the threshold dose model (15). There was no significant difference in the mean lesion diameter at the examined light dose between 5 and 15 min drug–light intervals. The mean lesion diameters with interstitial irradiation, including both time intervals, were 1.6 $\pm$ 0.1 cm (n = 4), 1.9 $\pm$ 0.4 cm (n = 7) and 3.0 $\pm$ 0.6 cm (n = 5) for 50, 100 and 200 J/cm, respectively. Some dissected sections showed hemorrhagic lesions encompassing the entire cross section around the treatment site and reaching the boundary of prostate gland. Periurethral hyperemia was noticed at all light doses. The surface of prostatic urethra was intact (see Fig. 3). One month after PDT, the prostate

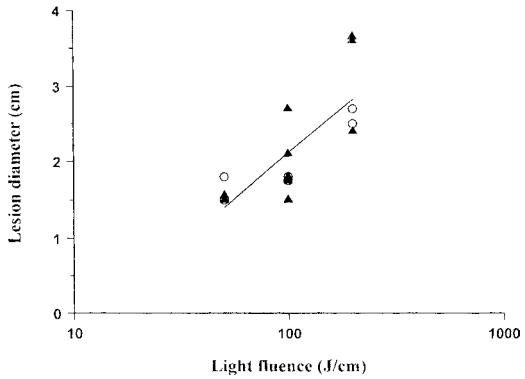

Figure 4. Correlation between lesion diameter and delivered light fluence from a single 1 cm interstitial diffusing fiber for 5 min (○) and 15 min (▲) time intervals between the end of drug administration and the start of light administration at 60–150 mW/cm. Each point represents one lobe. The log-linear regression line is shown ($R^2 = 0.67$).

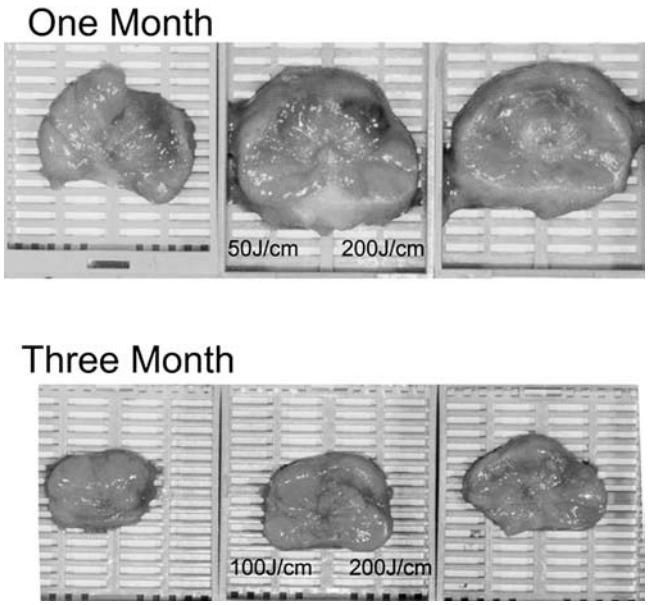

Figure 5. Dissected view of PDT-treated prostate (2 mg/kg, 50–200 J/cm and 15 min drug–light interval) after 1 and 3 months after treatment. Residual lesion and volume reduction are visible on the lobe receiving 200 J/cm after 1 month, whereas a large reduction in gland volume and scarring are visible after 3 months.

appeared pale and firm without signs of cavitation or collapse. Dissected sections of the lobe receiving 50 J/cm showed normal size and texture, whereas the lobes receiving 200 J/cm still showed a small area of residual lesions and reduction in gland volume (Fig. 5, top). Three months after PDT, the prostate retained its anatomical structure and shape, although a large reduction in gland volume was noticeable. The dissected sections showed normal texture and complete resolution of necrosis. The large reduction in gland volume and scarring were more obvious in lobes receiving 200 J/cm (Fig. 5, bottom). The residual lesions were still visible in lobes that received 200 J/cm. The urethra looked normal after 1 and 3 months.

One week after treatment, lesions from surface treatment were characterized by acute hemorrhagic necrosis with patchy subcapsular hyperemia and marked edema (see Fig. 3). The lesions were well-circumscribed necrosis, with the lesion size correlating well with light dose. The lesion depths were 1.8 ± 0.5 cm ($n = 3$) and 2.4 ± 0.7 cm ($n = 4$) for 100 and 200 J/cm^2, respectively. Some dissected sections showed necrotic lesions reaching the boundary of the prostate gland. The urethral structure appeared unaffected even when it lay within the PDT damage zone.

One week after PDT, the bladder, treated sections of colon and underlying rectum were examined. There was no visible damage on serosal or mucosal surface of the bladder or colon caused by scattered light or direct surface irradiation up to 40 J/cm^2. The area of colon receiving 80 J/cm^2 surface irradiation showed marked superficial hemorrhage. The ulceration corresponding to the irradiation field was clearly visible, but there was no apparent perforation or fistula.

Microscopic findings

On H&E sections examined by light microscopy, no abnormalities were seen in either the light-only control dog killed after 1 week or the drug-only control dog killed after 3 months. After 1 week, there were marked hemorrhagic necrosis and atrophy of the glandular tissue in the treated areas, with local hemorrhagic vasculitis, as seen in Fig. 6A. Necrotic material of glandular origin was seen in residual glandular lumen. Dilatation of glandular structures was noticeable in some specimens. The size of the lesions corresponded well with the hemorrhagic lesions seen on gross sections, with clear demarcation between the lesions and the adjacent normal tissue. At the apical and distal regions of the prostate, and beyond the visible PDT lesion boundary, normal glandular structures were well preserved, and some were surrounded by atrophic prostatic acinar tissue. Outside the necrotic area, the external striated urethral sphincter was unaffected. The fibromuscular region and connective tissue appeared to be damaged in the same way as the glandular tissue, characterized by diffuse and marked degeneration. Dyer's Verhoeff Variation stain showed that inside the PDT-treated area, the layers of collagenous and smooth muscle tissue of the capsule were preserved. But collagen fibrils in subsidiary ductal and acinar parts of the prostate were completely destroyed by PDT. At the PDT-induced severe necrotic region, vascular structures were completely destroyed. Thrombosis in regions with lesions indicated PDT-induced vascular damage. The prostatic capsule was unaffected.

In the 5 min drug–light interval group that received 50 J/cm interstitial irradiation, the necrotic lesions appeared different from that of the corresponding 15 min group. In the 5 min group, we observed more necrosis (40–60%) than atrophy (>20%) compared with less presence of necrosis (<10%) than atrophy (70%) in the 15 min group. Shorter drug–light intervals produced more necrotic lesions.

In cases in which the PDT lesion extended to or enclosed the urethra (100 and 200 J/cm interstitial irradiation), slight submucosal congestion and small areas of epithelial disruption were observed in some specimens (Fig. 6B). But even in these animals there were no clinical signs of urinary tract dysfunction, as reported by the attending veterinarian(s) during the postsurgical period.

Collagen stain revealed ongoing healing 1 month after PDT. After 1 month, the PDT-treated area showed resolving necrosis and fibrosis. Dense collagen deposition was found in the periurethral region. The area receiving 50 J/cm interstitial irradiation showed atrophic glandular tissue interposed with fibrosis. The

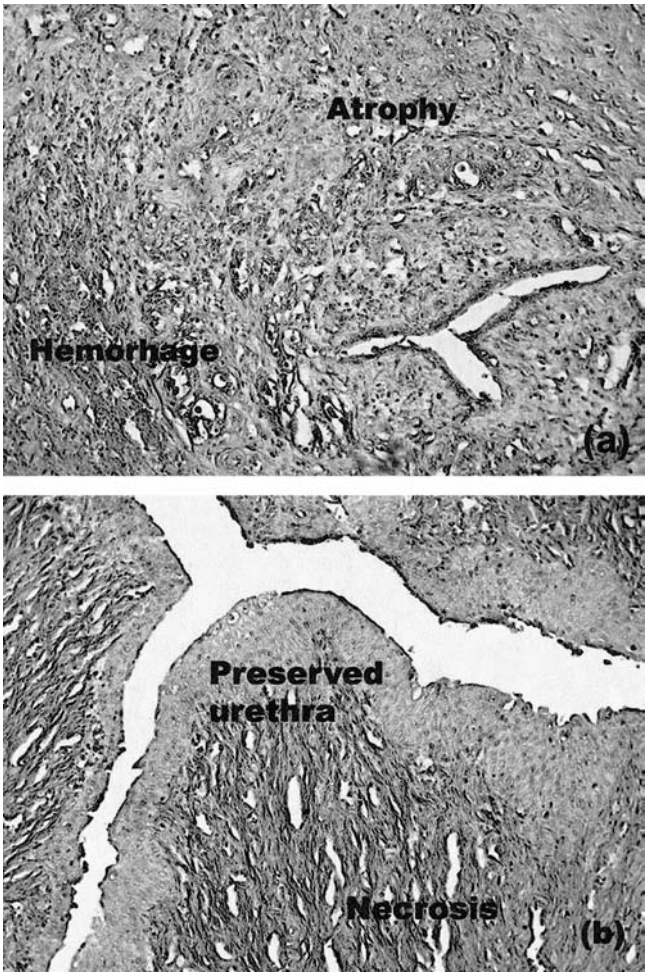

Figure 6. Microscopic features of prostate after 1 week after PDT (2 mg/kg, interstitial at 100 J/cm and 15 min drug–light interval). A: Hemorrhagic necrosis and atrophy of the prostate gland. B: Preserved urethra within the PDT-induced necrotic region (reduced from 100×).

area receiving 200 J/cm interstitial irradiation showed large bands of dense collagen deposition and small areas of residual hemorrhagic necrosis with little glandular regeneration. After 3 months, in PDT-treated lobes, necrosis had resolved completely. The necrotic zones induced by 100 and 200 J/cm interstitial irradiation shrunk further and were surrounded by bands of dense collagen and small areas of glandular regeneration. The urethral structures and fibromuscular and connective tissues of the capsule appeared normal after 1 and 3 months in all animals.

Slight hemorrhage and edematous and congestive reactions were observed in the serosal wall of the bladder irradiated directly at 40 J/cm^2, but there was no necrosis. No abnormalities caused by scattered light from irradiation of the prostate, either surface or interstitial, were observed at any light doses in the bladder wall or neck. Only slight inflammatory reactions were seen on the colon surface directly irradiated at 40 J/cm^2 PDT, and the mucosa and underlying colonic structures were well preserved. In the region of colon treated directly at 80 J/cm^2, there was marked hemorrhagic damage, with inflammation and mucosal ulceration 1 week after treatment. Full-depth necrosis was observed within the irradiation field. The treatment did not result in any form of colon perforation. With only scattered light, we observed no damages in the colon or rectum, as in the case of the bladder. Even in the three animals in which the colon was stitched directly to the prostate capsule to simulate more closely the human anatomy, we observed no histopathological changes in the region in contact with the prostate, except for mechanical damage caused by the suture.

DISCUSSION

For early-stage cancer confined within the prostate, standard therapy such as ionizing radiation or surgical prostatectomy does not differentiate between normal and cancerous prostate tissue. Rather, the goal is to ablate the entire organ. Thus, the ultimate goal of PDT in the management of prostate cancer is likely to be total ablation of the gland (15). Hence, the observations here are directly relevant to assessing the likely clinical utility of Tookad-based PDT of prostate cancer, assuming that the response of the malignant tissue will not be less than that of normal prostate. The high vascularity of tumor tissue makes it a good target for Tookad-PDT because the effects are believed to be primarily vascular (32). Furthermore, in locally recurrent cancer after radical radiation therapy, the normal prostate tissue becomes relatively avascular (33,34), which may confer some selective sensitivity of the neovascularized tumor.

It has been demonstrated in different tissues that PDT, in general, destroys glandular tissue (normal or neoplastic), yet has little effect on connective tissue. This is not completely true when a prostate is treated with Tookad-PDT; even if it largely retained its anatomical shape and structure. As shown with collagen staining, the healing process of normal prostate after Tookad-PDT is largely because of resolving and shrinking of necrotic tissue and rapid fibrosis, so that there should be minimal side effects compared with, for example, radical prostatectomy. Three months after PDT, small areas of glandular regeneration surrounded by bands of dense collagen were observed, indicating glandular cell proliferation from unaffected regions.

The potential of Tookad for this application of PDT is partly attributable to its being activated at a relatively long wavelength, with corresponding greater light penetration depth in the tissue. For example, compared with Photofrin-PDT, which we have investigated previously (6), for which Deff averaged 1.6 mm in normal prostate, the value found here at 763 nm was 4 mm. The deeper light penetration combined with the apparent high photodynamic effectiveness of Tookad means that much larger lesions than we were able to obtain previously with Photofrin-PDT at 630 nm (typically 1 cm diameter) can be produced. For example, lesions >3 cm diameter were obtained with a single interstitial diffusing fiber and a total light fluence of 100–200 J/cm. Such light fluences can be delivered in a time short enough to activate the drug while it is still in the vasculature but at a rate that does not induce significant tissue heating. The longer wavelength also makes the light distribution less sensitive to changes in tissue blood content: as seen in Fig. 2, there was little change in the local measured fluence rate during treatment in contrast to our findings with Photofrin at 630 nm where the fluence rate varied by more than 50% during an irradiation (6,15). This may also contribute to the contiguous and uniform lesions with Tookad, compared with the patchy distribution with Photofrin, although the drug distribution is also likely to play a significant role in this. Together, these features may make it possible to achieve complete tissue destruction throughout the prostate with a

relatively small number of interstitial sources (35). To do this reliably and safely, the drug and light dosimetry must be very accurately controlled and monitored. The variability of the lesion size at the higher light doses (Fig. 4) reinforces this point.

For reasons that are not understood, the PDT response of the normal bladder and colon appeared to be minimal compared with that of prostate tissue when treated with the same 40 J/cm^2 dose. There was considerable light scatter with each treatment, particularly at the higher fluences. For the largest PDT lesions (200 J/cm, interstitial fiber, 1.5 cm radius lesion, Deff $\sim$ 3 mm, assuming a few millimeter range for fluence buildup caused by backscatter), an upper estimate of the light fluence at the PDT lesion boundary is $\sim$20 J/cm^2, so that this is consistent with there being no colon or bladder damage caused by scattered light. The relative insensitivity of the colon or rectum and bladder should provide an additional safety margin that should allow aggressive treatment of the prostate with low risk of damage to these adjacent structures from scattered light. It is also encouraging that the effect on the urethra was minimal, both functionally in terms of micturition and from the gross and microscopic appearance, even when the prostatic urethra was within the treatment area and the immediately adjacent prostate tissue was destroyed. This was not the case with Photofrin (6,15) and may be related to the purely vascular targeting. The lack of urethral obstruction after PDT might have been related to the use of the steroid dexamethasone given to suppress the side effects of Cremophor.

In contrast to many photosensitizers being investigated clinically (36,37), Tookad-PDT is believed to be almost entirely vascularly mediated. The clearance of Tookad is very fast, with a plasma half-life in the mouse typically $<$1 h (A. Scherz, personal communication). Consistent with this, in several other tissues (including tumor and skin) studied in preclinical *in vivo* models (32), it has been observed that the light must be applied within a short time after (or even during) drug administration. In this regard, Tookad is similar to benzoporphyrin derivative monoacid ring ''a'' (Verteporfin; QLT, Vancouver, Canada), used for age-related macular degeneration, which is also activated while in the vascular system (38). For interstitial prostate PDT, this has the significant practical advantage that the drug and light may be administered in a single operative session. The fast clearance also improves the phototoxicity profile: in both rat and pig skin models, we have observed minimal potentiation of the UV response of normal skin and disappearance of any visible-light skin PDT response within a few hours of administration, even at high drug doses (B. C. Wilson, personal communication). Hence, the posttreatment patient management should be considerably simplified likely with little, if any, risk of skin damage, although this has yet to be confirmed in patients. Although the short drug–light time interval is a practical advantage, it also implies that the timing of the treatment must be very precise. In the prostate, we envisage that all preparations for the patient, including anesthesia and placement of light delivery fibers and any monitoring probes, will be completed before injecting the photosensitizer. The rate at which the drug is then delivered (which depends on its vehicle), the interval between the start of drug administration and light irradiation, and the light fluence rate must all be carefully optimized to ensure reproducibility of the treatment.

The Tookad formulation, administered intravenously, induced a marked drop in blood pressure in the dogs because of the presence of Cremophor, which is known to induce anaphylactoid reaction in this species (39). This side effect was easily controlled by premedication with antihistamine (i.v. Benadryl, 0.7–1.4 mg/kg) and steroids (dexamethasone, 2 mg SQ) and by adjustment of the anesthesia. Again, this will need to be incorporated into clinical protocols, although it is noted that other photosensitizers (40) and antineoplastic drugs in common use, such as paclitaxol, also use similar excipients (41).

In conclusion, these results suggest that Tookad may be well suited for PDT of prostate cancer. Clinical trials are currently being designed, initially for treatment of patients with localized recurrence of disease after radiation therapy failure. The initial drug and light doses and dose rates, and the drug–light time intervals, will be based on the findings reported above, together with other preclinical toxicology and PDT-response data (23,32, 35). Although this study and the initial trials are not predicated on there being an intrinsic selectivity for prostate cancer compared with normal prostate tissue, it will be of great interest to investigate whether this is the case.

Acknowledgements—This research was supported in part by Steba Biotech (France) and NIH grant PO1-CA43892.

REFERENCES

1. Boring, C. C., T. X. Squires and T. Tong (1994) Cancer statistics. *Can. J. Clin.* **44**, 7–26.
2. Paulson, D. F. (1988) Randomized series of treatment with surgery versus radiation for prostate adenocarcinoma. In *Consensus Development Conference on the Management of Clinically Localized Prostate Cancer* (Edited by R. I. Wittes), pp. 121–137. Government Printing Office, Washington, DC. [NIH publication no. 88-3005. NCI Monographs 7]
3. Lepor, H. and P. C. Walsh (1988) Long-term results of radical prostatectomy in clinically localized prostate cancer: experience at the John Hopkins Hospital. In *Consensus Development Conference on the Management of Clinically Localized Prostate Cancer* (Edited by R. I. Wittes), pp. 117–122. Government Printing Office, Washington, DC. [NIH publication no. 88-3005. NCI Monographs 7]
4. Catalona, W. J. (1994) Management of cancer of the prostate. *N. Eng. J. Med.* **331**, 996–1004.
5. Stamey, T. A. (1993) Irradiation as primary treatment for prostate cancer. *Am. Urol. Assoc. Today* **6**, 14.
6. Chen, Q. and F. W. Hetzel (1998) Laser dosimetry studies in the prostate. *J. Clin. Laser Med. Surg.* **16**, 9–12.
7. Onik, G. (2001) Image-guided prostate cryosurgery: state of the art. *Cancer Control* **8**, 522–531.
8. Chaussy, C. and S. Thuroff (2001) Results and side effects of high-intensity focused ultrasound in localized prostate cancer. *J. Endourol.* **15**, 437–440.
9. Henderson, B. W. and T. J. Dougherty (1992) How does photodynamic therapy work? *Photochem. Photobiol.* **55**, 145–157.
10. McPhee, M. S., C. W. Thorndyke, G. Thomas, J. Tulip, D. Chapman and W. H. Lakey (1984) Interstitial applications of laser irradiation in hematoporphyrin derivative-photosensitized Dunning R3327 prostate cancers. *Lasers Surg. Med.* **4**, 93–98.
11. Moore, R. B., J. D. Chapman, J. R. Mercer, R. H. Mannan, L. I. Wiebe, A. J. McEwan and M. S. McPhee (1993) Measurement of PDT-induced hypoxia in Dunning prostate tumors by iodine-123-iodoazomycin arabinoside. *J. Nucl. Med.* **34**, 405–411.
12. Momma, T., M. R. Hamblin, H. C. Wu and T. Hasan (1998) Photodynamic therapy of orthotopic prostate cancer with benzoporphyrin derivative: local control and distant metastasis. *Cancer Res.* **58**, 5425–5431.
13. Colasanti, A., A. Kisslinger, R. Liuzzi, M. Quarto, P. Riccio, G. Roberti, D. Tramontano and F. Villani (2000) Hypericin photosensitization of tumor and metastatic cell lines of human prostate. *J. Photochem. Photobiol. B: Biol* **54**, 103–107.
14. Xie, X., J. B. Hudson and E. S. Guns (2001) Tumor-specific and photodependent cytotoxicity of hypericin in the human LNCaP prostate tumor models. *Photochem. Photobiol.* **74**, 221–225.

15. Chen, Q., B. C. Wilson, S. D. Shetty, M. S. Patterson, J. C. Cerny and F. W. Hetzel (1997) Changes in *in vivo* optical properties and light distributions in normal canine prostate during photodynamic therapy. *Radiat. Res.* **147**, 86–91.
16. Lee, L. K., C. Whitehurst, M. L. Pantelides and J. V. Moore (1995) *In situ* comparison of 665 nm and 633 nm wavelength light penetration in the human prostate gland. *Photochem. Photobiol.* **62**, 882–886.
17. Lee, L. K., C. Whitehurst, M. L. Pantelides and J. V. Moore (1995) Interstitial photodynamic therapy in the canine prostate. *Br. J. Urol.* **80**, 898–902.
18. Selman, S. H., R. W. Keck and J. A. Hampton (1996) Transperineal photodynamic ablation of the canine prostate. *J. Urol.* **156**, 258–260.
19. Selman, S. H., D. Albrecht, R. W. Keck, P. Brennan and S. Kondo (2001) Studies of tin ethyl etiopurpurin photodynamic therapy of the canine prostate. *J. Urol.* **165**, 1795–1801.
20. Chang, S., G. A. Buonaccorsi, A. J. MacRobert and S. G. Bown (1997) Interstitial photodynamic therapy in the canine prostate with disulfonated aluminum phthalocyanine and 5-aminolevulinic acid-induced protoporphyrin IX. *The Prostate* **32**, 89–98.
21. Chang, S., G. Buonaccorsi, A. MacRobert and S. G. Bown (1996) Interstitial and transurethral photodynamic therapy of the canine prostate using meso-tetra-(m-hydroxyphenyl) Chlorin. *Int. J. Cancer* **67**, 555–562.
22. Hsi, R. A., A. Kapatkin, J. Strandberg, T. Zhu, T. Vulcan, M. Solonenko, C. Rodriguez, J. Chang, M. Saunders, N. Mason and S. Hahn (2001) Photodynamic therapy in the canine prostate using motexafin lutetium. *Clin. Cancer Res.* **7**, 651–660.
23. Scherz, A., Y. Salomon, H. Scheer and A. Brandis (1999) Palladium-substituted bacteriochlorophyll derivatives and use thereof. International PCT patent application no. PCT/IL99/00673.
24. Wagnieres, G., C. Hadjur, P. Grosjean, D. Braichotte, J. F. Savary, P. Monnier and H. van den Bergh (1998) Clinical evaluation of the cutaneous phototoxicity of 5,10,15,20-tetra(m-hydroxyphenyl)chlorin. *Photochem. Photobiol.* **68**, 382–387.
25. van Geel, I. P., H. Oppelaar, Y. G. Oussoren, M. A. van der Valk and F. A. Stewart (1995) Photosensitizing efficacy of MTHPC-PDT compared to Photofrin-PDT in the RIF1 mouse tumour and normal skin. *Int. J. Cancer* **60**, 388–394.
26. Chen, J. Y., N. K. Mak, J. M. Wen, W. N. Leung, S. C. Chen, M. C. Fung and N. H. Cheung (1998) A comparison of the photodynamic effects of temoporfin (mTHPC) and MC540 on leukemia cells: efficacy and apoptosis. *Photochem. Photobiol.* **68**, 545–554.
27. Regula, J., B. Ravi, J. Bedwell, A. J. MacRobert and S. G. Bown (1994) Photodynamic therapy using 5-aminolaevulinic acid for experimental pancreatic cancer-prolonged animal survival. *Br. J. Cancer* **70**, 248–254.
28. Bedwell, J., A. J. MacRobert, D. Phillips and S. G. Bown (1992) Fluorescence distribution and photodynamic effect of ALA-induced PpIX in the DMH rat colonic tumor model. *Br. J. Cancer* **65**, 818–824.
29. Barr, H., N. Krasner, P. B. Boulos, P. Chatlani and S. G. Bown (1990) Photodynamic therapy for colorectal cancer: a quantitative pilot study. *Br. J. Surg.* **77**, 93–96.
30. Sheeham, D. C. and B. B. Hrapchak (1987) *Theory and Practice of Histotechnology,* pp. 196–197. Battelle Press, Columbus, OH.
31. Selman, S. H. and R. W. Keck (1994) The effect of transurethral light on the canine prostate after sensitization with the photosensitizer tin (II) etiopurpurin dichloride: a pilot study. *J. Urol.* **152**, 2129–2132.
32. Zilberstein, J., S. Schreiber, M. C. Bloemers, P. Bendel, M. Neeman, E. Schechtman, F. Kohen, A. Scherz and Y. Salomon (2001) Anti vascular treatment of solid melanoma tumors with bacteriochlorophyll-serine-based photodynamic therapy. *Photochem. Photobiol.* **73**, 257–263.
33. Nadalini, V. F., C. Giglio, G. Bruttini, N. Positano, M. Fassone, L. Fasce, M. Medica, P. de Angelis, O. Fantacci, D. Scarpati and S. Ledda (1983) Histological follow-up after implantation of grains of I-125 for prostatic cancer. *J. Urol. (Paris)* **89**, 187–190. [In French]
34. Sheaff, M. T. and S. I. Baithum (1997) Effects of radiation on the normal prostate gland. *Histopathology* **30**, 341–348.
35. Chen, Q., Z. Huang, D. Luck, J. Beckers, P. Brun, B. C. Wilson, A. Scherz, Y. Salomon and F. W. Hetzel (2002) WST09 (TOOKAD) mediated photodynamic therapy as an alternative modality in treatment of prostate cancer. *Prog. Biomed. Opt. Imaging* **3**, 29–39. [see also *Proc. SPIE.* **4612**]
36. Adili, F., R. G. Statius van Eps and G. M. LaMuraglia (1999) Significance of dosimetry in photodynamic therapy of injured arteries: classification of biological responses. *Photochem. Photobiol.* **70**, 663–668.
37. Kurohane, K., A. Tominaga, K. Sato, J. R. North, Y. Namba and N. Oku (2001) Photodynamic therapy targeted to tumor-induced angiogenic vessels. *Cancer Lett.* **167**, 49–56.
38. Messmer, K. J. and S. R. Abel (2001) Verteporfin for age-related macular degeneration. *Ann. Pharmacother.* **35**, 1593–1598.
39. Bowers, V. D., S. Locker, S. Ames, W. Jennings and R. J. Corry (1991) The hemodynamic effects of Cremophor-EL. *Transplantation* **51**, 847–850.
40. Decreau, R., M. J. Richard, P. Verrando, M. Channon and M. Julliard (1990) Photodynamic activities of silicon phthalocyanines against achromic M6 melanoma cells and healthy human melanocytes and keratinocytes. *J. Photochem. Photobiol. B: Biol* **48**, 48–56.
41. Gelderblom, H., J. Verweij, K. Nooter and A. Sparreboom (2001) Cremophor EL: the drawbacks and advantages of vehicle selection for drug formulation. *Eur. J. Cancer* **37**, 1590–1598.